Inorganic Chemistry

Article

pubs.acs.org/IC

Time-Dependent Control of Hole-Opening Degree of Porous ZnO Hollow Microspheres

Nirmalya Tripathy,[†] Rafiq Ahmad,[†] Han-Sol Jeong,[‡] and Yoon-Bong Hahn*[,†,§,∥]

[†]Department of BIN Fusion Technology, [§]School of Semiconductor and Chemical Engineering, and [∥]Nanomaterials Processing Research Center, Chonbuk National University, Jeonju 561-756, Republic of Korea

[‡]Division of Applied Medicine, School of Korean Medicine, Pusan National University, 3-3 Beomeo-ri, Yangsan-si 626-870, Republic of Korea

ABSTRACT: Well-designed, monodispersed porous ZnO hollow microspheres with controlled hole-opening were successfully synthesized by a facile two-step solution route at low temperature. The hollow microspheres having average diameter of 3−4 μm showed time-dependent hole-opening, i.e. 4−100% for 15−75 min. The hole-opening percentage increases linearly with time until complete opening. The ZnO hollow microspheres also exhibited a high surface area (34 m^2 g^{-1}), a large pore volume (0.19 cm^3 g^{-1}) and an average pore diameter of 3.8 nm. A plausible growth mechanism for the formation of ZnO hollow microspheres was also proposed.

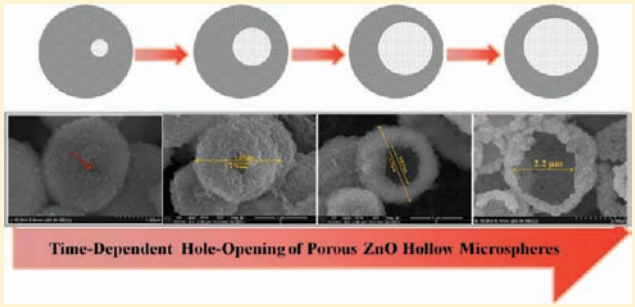

1. INTRODUCTION

Inorganic hollow structures of nanometer to micrometer dimensions exhibit large specific surface area, low density, nanostructured wall, good surface permeability and hollow nature, turning into a promising structure for various potential applications.[1,2] Zinc oxide (ZnO) is one of the most exciting materials for its versatile properties such as semiconducting (band gap of 3.37 eV), piezoelectric, biosafe and biocompatible nature. Owing to such properties ZnO can be efficiently used in various fields such as drug delivery vehicles,[3] fabrication of new photocatalyst,[4] UV light-emitting devices,[5] room temperature UV lasers,[6] chemical and biological sensors,[7,8] microsensors,[9] decontamination agents,[10] and so on. Especially, ZnO hollow microspheres, due to a porous nature and hollow interior, can be used as efficient medicine carriers with high medicine loadings and delay in the drug release process. The low density and high surface area of the hollow spheres also make them desirable as fillers for modifying the properties of resins, enhancing device performance by increased enzyme loading showing high catalytic activities, and prolongating the time of catalytic reactions. To synthesize micro-hollow ZnO spheres, two routines are available, i.e. solution-based and gas-phase methods. The former focuses on template-assisted technology employing polystyrene spheres,[11] silica spheres,[12] carbon spheres,[13] liquid droplets,[14] emulsion droplets, micelles,[15,16] ethanol droplets,[17] etc. The latter is based on direct oxidation of zinc precursors on different substrates at high temperatures, for example, thermal evaporation of metallic zinc powder in the presence of oxygen at 600 °C[18] and 800 °C.[19] However, all these methods were not able to control the hole-opening degree, which is crucial for high drug loading as well as for device performance.

In this work, to control the hole-opening we demonstrate a simple two-step growth method for well-designed, monodispersed porous ZnO hollow microspheres without the use of any templates, catalysts and/or chemicals. For more elaborated study of the growth mechanism of ZnO hollow microspheres, the effects of time and annealing temperature on the hole-opening percentage are discussed in detail.

2. EXPERIMENTAL SECTION

ZnO microstructures with hollow interiors were successfully synthesized by a simple, rapid, low temperature solution method using zinc nitrate hexahydrate [$Zn(NO_3)_2{\cdot}6H_2O$], hexamethylenetetramine [HMTA; $C_6H_{12}N_4$], sodium citrate tribasic [$C_6H_5Na_3O_7{\cdot}2H_2O$] and ammonia solution [$NH_4OH$] in the two-step process. All of the chemicals were used as received from Sigma Aldrich without any further purification. In the first step of the synthesis of ZnO spheres (step I), an equimolar ratio of zinc nitrate hexahydrate (0.02 M) and HMTA (0.02 M) was dissolved in 100 mL of deionized water with subsequent addition of sodium citrate tribasic (0.005 M) with stirring at room temperature. After a clear solution was obtained, it was then transferred to a three-necked refluxing reactor with the Si (100) substrate and refluxed at 80 °C for 1 h. Further the white colored products were found to be deposited on the Si (100) substrate, which was used for the next step.

In the second step of the synthesis of ZnO hollow microspheres (step II), an equimolar ratio of zinc nitrate hexahydrate (0.01 M) and HMTA (0.01 M) was dissolved in a beaker containing 100 mL of distilled water. In the same beaker, sodium citrate tribasic (0.002 M) was added and whole solution was stirred for 10 min. Once again the above solution was transferred to the three-necked refluxing reactor with the step I resulted products on the Si substrate and heated at 80

Received: October 18, 2011
Published: December 29, 2011

dx.doi.org/10.1021/ic2022598 | *Inorg. Chem.* 2012, 51, 1104−1110

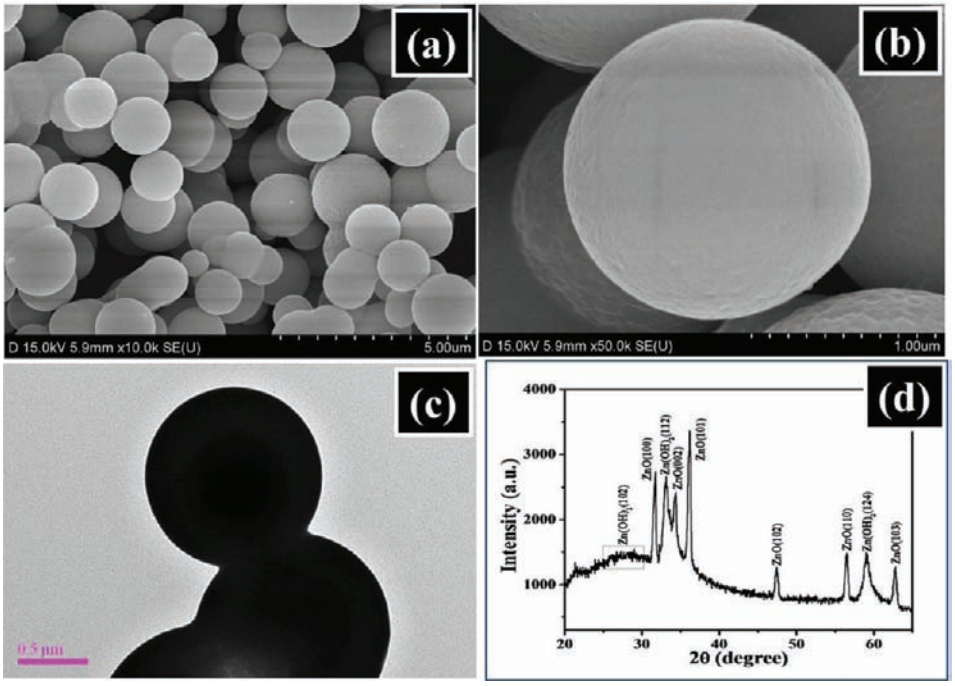

Figure 1. (a) Low and (b) high magnification FESEM images, (c) TEM image and (d) XRD pattern of the ZnO-$Zn(OH)_2$ microspheres formed in step I.

°C with varying reaction time, i.e. 15, 30, 45, 60, 75 min. Moreover, the acidity of solution was maintained at pH = 9 by the addition of NH_4OH, and the reaction temperature (80 °C) and the concentration of all the precursors was kept constant. Finally, the time-dependent step II produced white colored precipitates on the substrate, i.e. hollow microstructures, which were washed several times with DI water for the removal of impurities and dried at room temperature for further characterization.

The structural morphology of as-grown ZnO hollow microstructures was examined by field emission scanning electron microscopy (FESEM) transmission electron microscopy (TEM), and high-resolution TEM (HRTEM). The crystallinity and crystal phases of as-synthesized ZnO hollow spheres were examined by X-ray diffractometer (XRD) measured with Cu Kα radiation (λ = 1.54178 Å) in the range of 20−80° with 8°/min scanning speed. The optical properties were characterized by Raman-scattering measurements with Ar^+ (513.4 nm) as the exciton source. Nitrogen adsorption−desorption analysis was performed using an ASAP 2010 analyzer at 77 K. The pore size distribution was determined from the adsorption isotherm curves using the Barrett−Joyner−Halenda (BJH) method.

3. RESULTS AND DISCUSSION

3.1. Structural Characterization of Hollow ZnO Microspheres. Figure 1 shows typical images of FESEM (a, b), TEM (c) and XRD pattern (d) of the ZnO-$Zn(OH)_2$ composite spheres formed in step I. The SEM images exhibit uniformly distributed ZnO-$Zn(OH)_2$ spheres having smooth surfaces on the outer side with diameter of 1−1.5 μm, grown in large quantity on substrate. The TEM image (c) of the spherical particle further confirms that the spheres are solid and smooth on the outer surface. The XRD pattern (d) reveals that the step I products are composites of wurtzite ZnO and $Zn(OH)_2$. All the peaks of (100), (002), (101), (102), (110), and (103) are attributed to wurtzite ZnO structure according to JCPDS 36-1451.[20,21] In contrast, three peaks of (102), (112) and (124) correspond to diffraction peaks of $Zn(OH)_2$ in accordance with (JCPDS 89-0138).[22]

Figure 2 shows typical FESEM images (a, b), TEM images (c) and HRTEM (d), energy dispersive X-ray spectrometry (EDX) spectrum (e), and Raman scattering spectrum (f) of the ZnO hollow spheres synthesized in step II at 80 °C for 1 h. SEM images show a well-dispersed large quantity of hollow ZnO microspheres with average diameter of 3−4 μm and hole-opening diameter of 2.2−2.6 μm. The clear view of the hollow-shaped structure (b) shows the regular shape of spheres along with the inside hollow nature. Additionally the porous nature of the microspheres is also observed from both the surface and inside. Interestingly, it seems that several nanosheets were arranged forming such porous hollow spheres. The TEM image (c) clearly shows the porous spherical-shaped microstructures with a hollow interior and nanostructured wall. The corresponding selected area electron diffraction (SAED) pattern (inset of c) indicates the polycrystalline nature of the as-synthesized microstructures. Also the HRTEM image (d) taken from the edge of a single ZnO microsphere further confirms the porous nature and the nanostructured wall consisting of small nanoparticles (inset of d). The EDX spectrum (e) demonstrates that the products are made of Zn and O only and the atomic ratio of Zn to O is about 1:1. The crystallinity of ZnO microspheres was further examined by Raman scattering (f), which shows a clear and prominent peak at 439 cm^{-1}, attributed to Raman-active optical-phonon E_2 mode for wurtzite ZnO.[23] It is worthwhile to note that we did not observe any significant peak at 586 cm^{-1} attributed to the E_1 (LO) mode, associated with oxygen vacancies, interstitial zinc, and their complexes.[24]

3.2. Effect of Reaction Time on Hole-Opening. To examine the effect of reaction time on the hole-opening degree of ZnO microspheres during step II, time-dependent experiments have been performed by keeping other reaction parameters constant. Figure 3 shows the low (left) and high (middle) magnification FESEM images and TEM images (right) of the samples synthesized for 15 min (a), 30 min (b),

dx.doi.org/10.1021/ic2022598 | Inorg. Chem. 2012, 51, 1104−1110

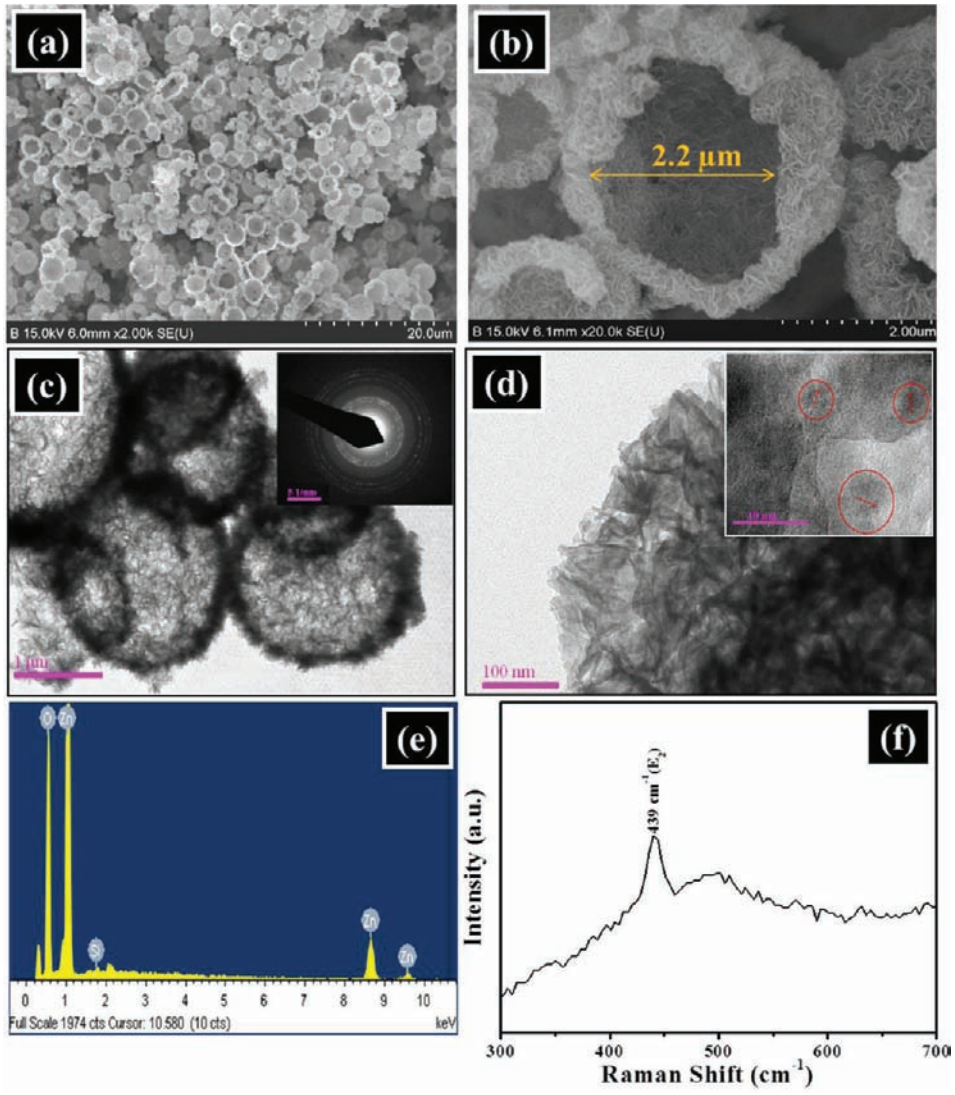

Figure 2. (a) Low and (b) high magnification FESEM images, (c) TEM and (d) HR-TEM images, (e) EDX and (f) Raman scattering spectra of as-grown hollow ZnO microspheres via step II for 1 h at 80 °C and pH = 9. The insets in (c) and (d) show SAED pattern and magnified HR-TEM image, respectively.

45 min (c), 60 min (d), and 75 min (e), respectively. In the pioneer stage for 15 min, spherical-shaped microstructures were formed and the initiation of hole-opening on the surface was observed, marked by the red arrows (a1, a2). In the TEM image (a3), a strong contrast difference with a dark edge and relatively light inner center shows the initiation of hole opening along with the inside core. As the reaction time increased from 15 to 30 min, a clear pore opening of ~400 nm was observed (b1, b2). The TEM image (b3) clearly shows the contrast difference with the dark edge and relatively light inner center becoming stronger and thereby providing evidence for an increase in hole-opening. With further increase of the reaction time from 30 to 45 min, the hole size of the microsphere increases to ~840 nm without affecting the actual size of the microspheres (c1−c3). A more clear change is observed with further increas of the time to 60 min, showing well-dispersed microspheres with an increased pore opening of 2.2 μm (d1−d3). At this point of reaction time, the ZnO microstructure maintains a spherical shape (3−4 μm) along with the appropriate opening degree of ~74% (also see Figure 4), thereby considered as the optimum growth time for the synthesis of ZnO hollow microspheres with a large surface area. By further increasing the reaction time to 75 min a full opening (~ 100%) is obtained, but most microspheres are distorted (e1−e3). Figure 4 represents the histogram of time-dependent hole-opening percentage (η) in ZnO hollow microspheres (top) and the linear plot of η vs reaction time (bottom). The hole-opening percentage at different reaction times was calculated simply from η (%) = $d_h/D_m \times 100$ (%), where d_h and D_m represent the diameters of hole-opening and ZnO microsphere, respectively. After the hole-opening started, a linear increase in the hole-opening degree from 4 to 100% was observed with increasing the reaction time from 15 to 75 min, which is consistent with FESEM and TEM images (see Figure 3). The correlation coefficient of the linearity with time is R^2 = 0.9955, indicating that growth time is a most important parameter to control the hole-opening of ZnO microspheres.

3.3. Effect of Annealing Temperature. Figure 5 shows the XRD patterns (a) and FESEM images (b1−b5) of ZnO hollow microspheres after annealing under varying temperature from 100 to 500 °C for 2 h. All the reflection peaks from samples before and after annealing were indexed to wurtzite

dx.doi.org/10.1021/ic2022598 | Inorg. Chem. 2012, 51, 1104−1110

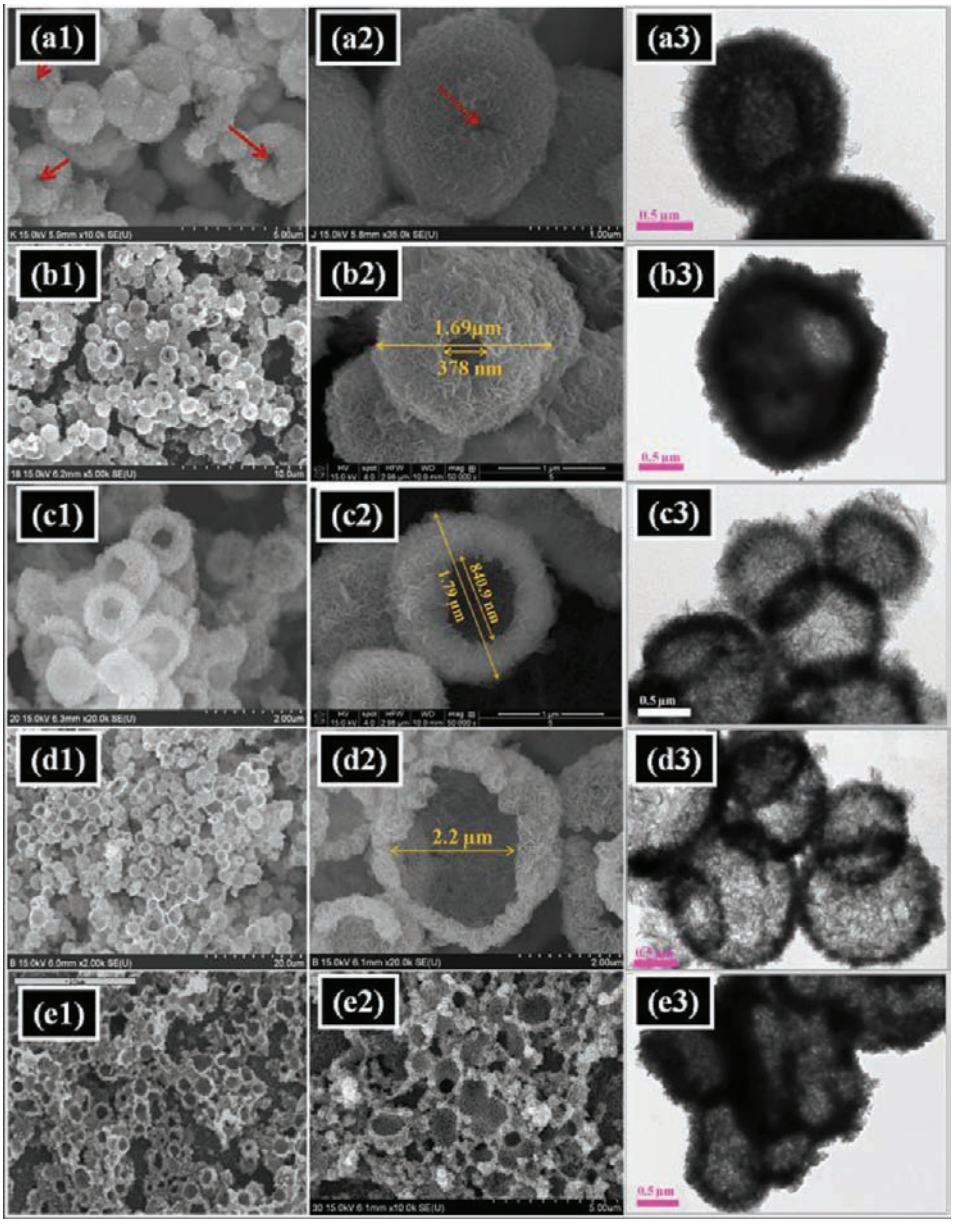

Figure 3. Time-dependent hole-opening of ZnO microspheres: low (left) and high (middle) magnification FESEM images and TEM images (right) of the samples synthesized at 80 °C and pH = 9 for different reaction times: 15 min (a), 30 min (b), 45 min (c), 60 min (d), and 75 min (e), respectively.

ZnO (JCPDS No. 36-1451). Compared with the XRD pattern of the ZnO-$Zn(OH)_2$ composite formed in step I (see Figure 1d), no diffraction peaks for $Zn(OH)_2$ were observed from the products of step II. With increasing the annealing temperature the intensities of the diffraction peaks become more prominent and stronger (also see fwhm inset of a). It is interesting to see that an increase in annealing temperature does not have any significant effect either on the sphere size or on the hole-opening degree as shown in the respective FESEM images (b1–b5).

3.4. Surface Area and Pore Size Distribution. Figure 6 shows (a) the pore volume and (b) the pore size distribution of the ZnO hollow microspheres synthesized at 80 °C for 60 min in step II, which were analyzed from N_2 adsorption–desorption isotherms based on the BJH (Barrett–Joyner–Halenda) model. The ZnO hollow microspheres exhibit high surface area, large pore volume, and narrow pore size distribution. At high P/P_0 between 0.4 and 1.0, the samples exhibit a type H1 hysteresis loop (IUPAC classification) indicating the porous nature of ZnO hollow microspheres. The BET (Brunauer–Emmett–Teller) surface area and the pore volume are found to be 34 m^2 g^{-1} and 0.19 cm^3 g^{-1} respectively. The pore size distribution curve of the ZnO hollow microspheres suggests a narrow pore size distribution ranging from 2 to 25 nm with an average pore diameter of 3.8 nm.

3.5. Growth Mechanism for the Formation of Hollow ZnO Microspheres. Based on the morphological changes observed in the time-dependent growth of ZnO hollow microspheres, a two-step growth mechanism was proposed as illustrated in Figure 7. In the first step (step I) with the solution containing zinc nitrate hexahydrate, HMTA and sodium citrate tribasic (i), the nucleation and growth of composite ZnO/$Zn(OH)_2$ units take place on substrate (ii). It is predicted that, at an early stage of step I, the reaction produces $Zn(OH)_2$

dx.doi.org/10.1021/ic2022598 | Inorg. Chem. 2012, 51, 1104–1110

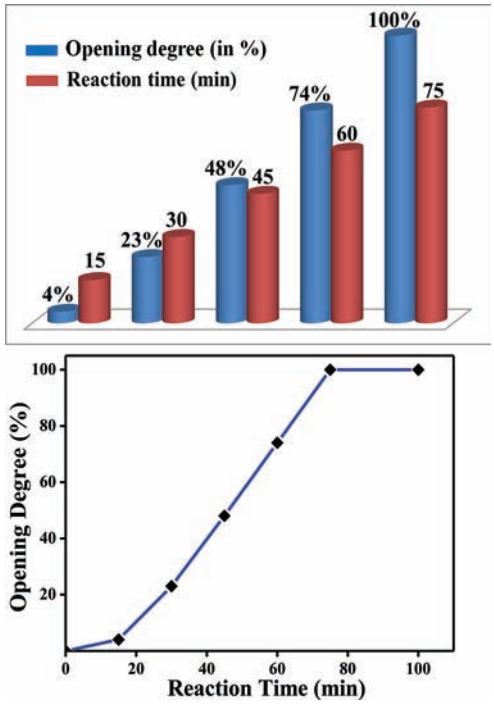

Figure 4. (a, top) Histogram showing the hole-opening percentage of ZnO hollow microspheres at different reaction times and (b, bottom) linear plot of η vs time.

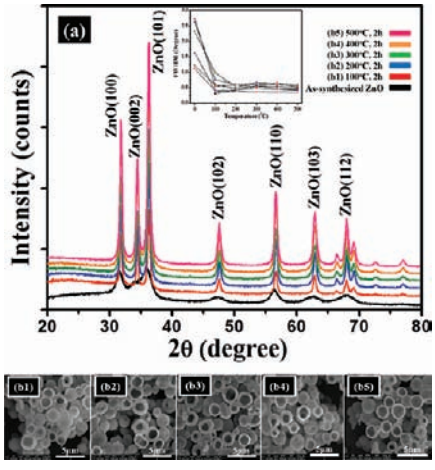

Figure 5. (a) XRD patterns of as-synthesized and annealed ZnO hollow microspheres at different temperatures from 100 to 500 °C, with fwhm in inset. (b) FESEM images of ZnO hollow microspheres annealed for 2 h at 100 °C (b1), 200 °C (b2), 300 °C (b3), 400 °C (b4) and 500 °C (b5), respectively.

nuclei, which initially serves as the basic building units for the formation of solid sphere. HMTA provides two things, i.e. first it hydrolyzes and produces OH^- ions slowly (it is reported that, at elevated temperature, HMTA can be hydrolyzed in the distilled water and slowly generate the OH^- ions)[25] by the chemical reactions mentioned in Figure 7. Then the free OH^- ions meet Zn^{2+} ions to produce $Zn(OH)_2$ nuclei (iii) on substrate. In addition, the presence of citrate ions from the trisodium citrate plays a critical role as a structure-directing agent. The citrate ions in solution suppress the growth of ZnO/$Zn(OH)_2$ crystal in all directions (iv), thereby giving rise to spherical shape morphology (v). Tian et al. reported that a very small quantity of citrate anion can effectively slow down the

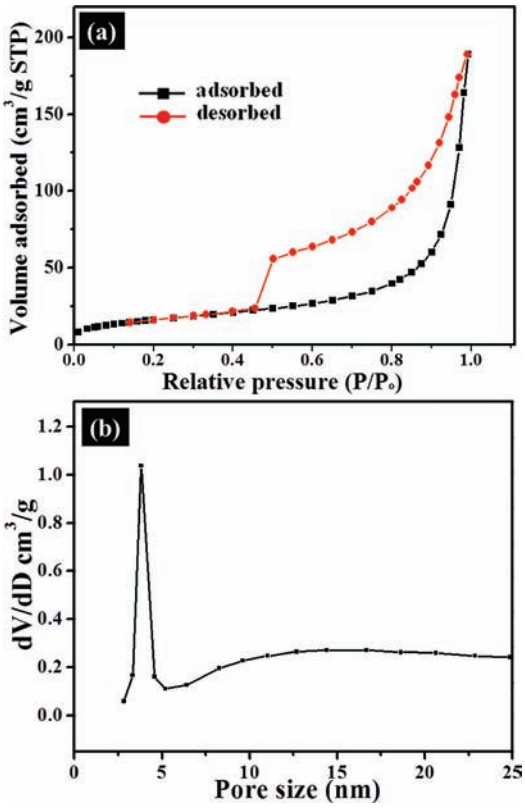

Figure 6. (a) Nitrogen adsorption–desorption isotherm and (b) BJH pore size distribution curve of the ZnO hollow microspheres.

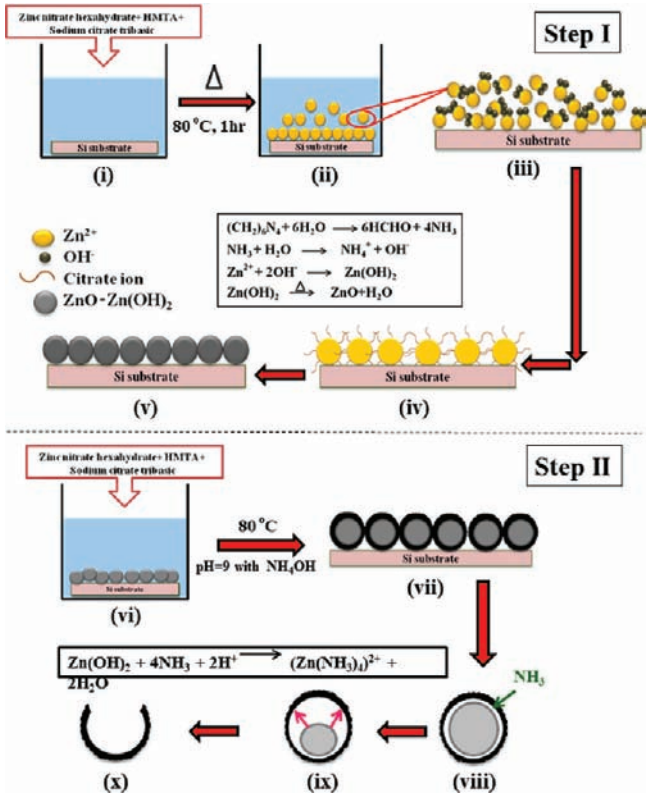

Figure 7. Schematic illustration of growth mechanism for the formation of ZnO hollow microspheres.

dx.doi.org/10.1021/ic2022598 | Inorg. Chem. 2012, 51, 1104–1110

crystal growth along the ⟨0001⟩ orientation.[26] In the second stage (step II), the microspheres on the substrate formed in step I were transferred into a solution containing zinc nitrate hexahydrate, HMTA, sodium citrate tribasic with pH = 9 maintained by addition of ammonium hydroxide. During the initial stage of step II, another layer of ZnO-$Zn(OH)_2$ is deposited on the surface of the step I resulted ZnO-$Zn(OH)_2$ composite microspheres, i.e. the formation of core−shell type microspheres (vii). With the addition of ammonium hydroxide, it reacts with $Zn(OH)_2$ and penetrates through the outer layer of the microsphere forming a microporous structure. Further it etches $Zn(OH)_2$ inside the microsphere, thereby resulting in the formation of a hollow interior by destroying the inner core without affecting the overall shape of the ZnO microsphere (ix). It is worthwhile to note that if we put the step I resulted products in NH_4OH solution directly, the NH_3 causes complete breakdown of the microspheres. This means that the ZnO-$Zn(OH)_2$ shell formed during the initial stage of step II plays a crucial role in the formation of hollow microspheres. The possible chemical reactions occurring during step II mentioned above are as follows:

$$ZnO(s) + NH_3(aq) + 2H^+(aq) \rightarrow Zn(NH_3)^{2+}(aq) + H_2O(l),\ \Delta G^\circ = -15.51\ kJ/mol \quad (1)$$

$$ZnO(s) + 2NH_3(aq) + 2H^+(aq) \rightarrow Zn(NH_3)_2{}^{2+}(aq) + H_2O(l),\ \Delta G^\circ = 58.63\ kJ/mol \quad (2)$$

$$ZnO(s) + 3NH_3(aq) + 2H^+(aq) \rightarrow Zn(NH_3)_3{}^{2+}(aq) + H_2O(l),\ \Delta G^\circ = 132.78\ kJ/mol \quad (3)$$

$$Zn(OH)_2(s) + 4NH_3(aq) + 2H^+(aq) \rightarrow Zn(NH_3)_4{}^{2+}(aq) + 2H_2O(l),\ \Delta G^\circ = -151.1\ kJ/mol \quad (4)$$

Comparing Gibbs free energy (i.e., ΔG° at 298 K) for each reaction, we can see that the most favorable chemical reaction to be involved in initiating and enlarging the hole-opening process is $Zn(OH)_2 + 4NH_3 + 2H^+ \rightarrow Zn(NH_3)_4{}^{2+} + 2H_2O$, $\Delta G^\circ = -151.1$ kJ/mol. This reaction probably prevails as the overall reaction until the reaction time for 100% opening with complete removal of $Zn(OH)_2$; but with longer time than for complete opening, the ZnO layer begins to partly dissolve by eq 1, thus resulting in distorting or degrading the microspheres, which is evidenced by SEM (Figure 3e1−e3).

In addition, it is worthwhile to understand the formation mechanism of nanosheets that consist of the shell of ZnO microspheres. The growth velocities of the ZnO crystals in different directions are known as $V_{\langle 0001\rangle} > V_{[01\bar{1}0]} > V_{[01\bar{1}1]} > V_{[000\bar{1}]}$ under hydrothermal conditions.[27] Therefore, the preferential growth orientation of ZnO nanostructures is the *c*-axis along the ⟨0001⟩ direction, resulting in nanowire-type morphologies. However, under certain circumstances (for example, addition of NH_4OH in the citrate anion containing solution in our experiments) the growth in the ⟨0001⟩ direction is probably suppressed and thus the ZnO crystals grow along the six directions of <01$\bar{1}$0> to form sheetlike morphology.[28] It is also known that the crystal growth along the ⟨0001⟩ direction is retarded by a small amount of citrate anions.[26] Due to such growth behavior, many ZnO nanosheets are formed and joined to each other, and thus form the nanosheet networks. The SEM and TEM observations of the as-synthesized ZnO microspheres of which shells are composed of nanosheet networks (see Figures 2 and 3) support such a conclusion. However, further study is needed to precisely understand the detailed formation mechanism of the nanosheets.

4. CONCLUSIONS

A simple, cost-effective, solution-based method for synthesizing ZnO hollow microspheres was developed. The hollow microspheres exhibited an average diameter of 3−4 μm with time-dependent hole-opening degree, i.e. 4−100% for 15−75 min. It was observed that the reaction time has a prominent impact on the hole-opening degree of the as-synthesized microspheres. The porous ZnO hollow microspheres also showed a high surface area (34 $m^2\ g^{-1}$), a large pore volume (0.19 $cm^3\ g^{-1}$) and an average pore diameter of 3.8 nm. Finally a plausible two-step growth mechanism for the formation of ZnO hollow microspheres was proposed. The most favorable chemical reaction involved in initiating and enlarging the hole-opening process is $Zn(OH)_2 + 4NH_3 + 2H^+ \rightarrow Zn(NH_3)_4{}^{2+} + 2H_2O$. This reaction is responsible for 100% opening and complete removal of $Zn(OH)_2$.

AUTHOR INFORMATION

Corresponding Author

*E-mail: ybhahn@chonbuk.ac.kr.

ACKNOWLEDGMENTS

This work was supported in part by the Pioneer Research program (2011-0001663) and by the World Class University program (R31-20029) funded from Korean government (MEST). Authors also thank KBSI, Jeonju branch, for SEM and Mr. Jong-Gyun Kang, Centre for University Research Facility (CURF), for quality TEM image.

REFERENCES

(1) Qing, P.; Yajie, D.; Yadong, L. *Angew. Chem., Int. Ed.* **2003**, *42*, 3027.
(2) Bertling, J.; Blomer, J.; Kummel, R. *Chem. Eng. Technol.* **2004**, *27*, 829.
(3) Yuan, Q.; Hein, S.; Misra, R. D. K. *Acta Biomater.* **2010**, *6*, 2732.
(4) Vora, J. J.; Chauhan, S. K.; Parmar, K. C.; Vasava, S. B.; Sharma, S.; Bhutadiya, L. S. *E-J. Chem.* **2009**, *6*, 531.
(5) Konenkamp, R.; Word, R. C.; Godinez, M. *Nano Lett.* **2005**, *5*, 2005.
(6) Cao, H.; Xu, J. Y.; Zhang, D. Z.; Chang, S. H.; Ho, S. T.; Seeling, E. W.; Liu, X.; Chang, R. P. H. *Phys. Rev. Lett.* **2000**, *84*, 5584.
(7) Umar, A.; Rahman, M. M.; Hahn, Y. B. *Talanta* **2009**, *78*, 284.
(8) Umar, A.; Rahman, M. M.; Kim, S. H.; Hahn, Y. B. *J. Nanosci. Nanotechnol.* **2008**, *8*, 3216.
(9) Xu, J. Q.; Pan, Q. Y.; Shun, Y. A.; Tian, Z. Z. *Sens. Actuators, B* **2000**, *66*, 277.
(10) Muthukumar, S.; Gorla, C. R.; Emanetoglu, N. W.; Liang, S.; Lu, Y. *J. Cryst. Growth* **2001**, *225*, 197.
(11) Deng, Z.; Chen, M.; Gu, G.; Wu, L. *J. Phys. Chem. B* **2008**, *112*, 16.
(12) Xu, X.; Asher, S. A. J. *Am. Chem. Soc.* **2004**, *126*, 7940.
(13) Sun, X. M.; Li, Y. D. *Angew. Chem., Int. Ed.* **2004**, *43*, 3827.

(14) Huang, J.; Xie, Y.; Li, B.; Qian, Y.; Zhang, S. *Adv. Mater.* **2000**, *12*, 808.
(15) Yang, H. G.; Zeng, H. C. *Angew. Chem.* **2004**, *116*, 5318.
(16) Li, Y.; Shi, J.; Hua, Z.; Che, H.; Ruan, M.; Yan, D. *Nano Lett.* **2003**, *3*, 609.
(17) Jiang, Z. Y.; Xie, Z. X.; Zhang, X. H.; Lin, S. C.; Xu, T.; Xie, S. Y.; Huang, R. B.; Zheng, L. S. *Adv. Mater.* **2004**, *16*, 904.
(18) Umar, A.; Hahn, Y. B. *Appl. Surf. Sci.* **2008**, *254*, 3339.
(19) Fan, H. J.; Scholz, R.; Kolb, F. M.; Zacharias, M.; Gosele, U. *Solid State Commun.* **2004**, *130*, 517.
(20) Khan, A.; Jadwisienczak, W. M.; Kordesch, M. E. *Physica E* **2006**, *33*, 331.
(21) Wu, X.; Li, K.; Wang, H. *J. Hazard. Mater.* **2010**, *174*, 573.
(22) Kusaba, K.; Kikegawa, T. *Solid State Commun.* **2008**, *148*, 382.
(23) Li, L.; Yang, H.; Qi, G.; Ma, J.; Xie, X.; Zhao, H.; Gao, F. *Chem. Phys. Lett.* **2008**, *455*, 93.
(24) Xu, X. L.; Lau, S. P.; Chen, J. S.; Che, G. Y.; Tay, B. K. *J. Cryst. Growth* **2001**, *223*, 201.
(25) Govender, K.; Boyle, D. S.; Kenway, P. B.; O'Brien, P. *J. Mater. Chem.* **2004**, *14*, 2575.
(26) Tian, Z. R.; Voigt, J. A.; Liu, J.; Mckenzie, B.; Mcdermott, M. J.; Cygan, R. T.; Criscenti, L. J. *Nat. Mater.* **2003**, *2*, 821.
(27) Li, W.-J.; Shi, E.-W.; Zhong, W.-Z.; Yin, Z.-W. *J. Cryst. Growth* **1999**, *203*, 186.
(28) Umar, A.; Hahn, Y. B. *Nanotechnology* **2006**, *17*, 2174.